Am J Cancer Res 2024;14(5):2507-2522
www.ajcr.us /ISSN:2156-6976/ajcr0155474

Original Article

RSAD2, a pyroptosis-related gene, predicts the prognosis and immunotherapy response for colorectal cancer

Yunxiao Li[1*], Qianqian Cui[2*], Bin Zhou[3], Jiayu Zhang[1], Rong Guo[1], Yanyan Wang[2], Xinhua Xu[1]

[1]Department of Oncology, The First College of Clinical Medical Science, China Three Gorges University/Yichang Central People's Hospital, Yichang 443000, Hubei, China; [2]Department of Pharmacy, The First College of Clinical Medical Science, China Three Gorges University/Yichang Central People's Hospital, Yichang 443000, Hubei, China; [3]Union Hospital, Tongji Medical College, Huazhong University of Science and Technology, Wuhan 430000, Hubei, China. [*]Equal contributors.

Received January 16, 2024; Accepted April 22, 2024; Epub May 15, 2024; Published May 30, 2024

Abstract: Colorectal cancer (CRC) is among the most prevalent malignant tumors, known for its high heterogeneity. Although many treatments and medications are available, the long-term survival rate of CRC patients is far from satisfactory. Pyroptosis is closely related to tumor progression. This study aimed to identify pyroptosis-related genes (PRGs) and candidate biomarkers to predict the prognosis of CRC patients. Used bioinformatics, we identified PRGs and subsequently screened 288 co-expression genes between pyroptosis-related modules and differentially expressed genes in CRC. Among these hub genes, we selected the top 24 for further analysis and found that Radical S-Adenosyl Methionine Domain Containing 2 (RSAD2) was a novel biomarker associated with the progression of CRC. We developed a risk model for RSAD2, which proved to be an independent prognostic indicator. The receiver operator characteristic analysis showed that the model had an acceptable prognostic value for patients with CRC. In addition, RSAD2 also affects the tumor immune microenvironment and prognosis of CRC. We further validated RSAD2 expression in CRC patients using RT-qPCR and the role of RSAD2 in pyroptosis. Taken together, this study comprehensively assessed the expression and prognostic value of RSAD2 in patients with CRC. These findings may offer a new direction for early CRC screening and development of future immunotherapy strategies.

Keywords: Colorectal cancer, pyroptosis, RSAD2, tumor microenvironment, prognosis

Introduction

Colorectal cancer (CRC) is the second leading cause of cancer-related death [1, 2]. With the aging of population in China and lifestyle changes, the incidence and mortality rates of CRC are gradually increasing and show a trend toward younger ages. Early screening and accurate diagnosis are critical for reducing cancer-related mortality. According to the American Cancer Society, cancer deaths in the United States have dropped by nearly one-third, largely due to early screening [3]. Therefore, biomarkers for the early detection and screening of CRC are garnering increasing attention.

Pyroptosis, a new form of programmed cell death, leads to cleavage of gasdermin D (GSDMD) and activates inflammatory factors [4, 5]. Substantial evidence suggests that pyroptosis plays a critical role in immune response and tumor progression, including CRC [6-8]. Long-term chronic pyroptosis of cancer cells triggered by the tumor microenvironment (TME) is more likely to promote cancer progression [9]. Studies have showed that GSDME-mediated pyroptosis promotes the development of CRC by releasing high-mobility group box protein 1 (HMGB1), which induces tumor cell proliferation and the expression of proliferating nuclear antigen through the ERK1/2 pathway [10]. Pyroptosis in tumor cells leads to a powerful immune response and significant tumor regression, highlighting its dual role in promoting and suppressing tumors. The antitumor effects of pyroptosis are largely due to GSDMD-induced pore formation, which facilitates the release of pro-inflammatory cytokines and immunogenic substances following cell rupture [11, 12]. Although pyroptosis has potential in the early diagnosis and treatment of cancers, markers specifically related to pyroptosis in cancer are still insufficiently characterized.

https://doi.org/10.62347/RGJO6884

Emerging evidence indicates crosstalk between pyroptosis and TME [13, 14], which is known to affect tumor development and progression. TME participates in immune cell activation and recruitment, which induces the progression of tumors, including CRC. In contrast, TME can also be a site of local inflammation that contributes to systemic inflammation. During pyroptosis, activated IL-1β is released from GSDM pores to influence the TME. IL-1β induces maturation of dendritic cells (DCs) and promotes the differentiation of monocytes into DCs and macrophages [15].

In this study, we identified pyroptosis-related genes (PRGs) through bioinformatic analysis and found that Radical S-Adenosyl Methionine Domain Containing 2 (RSAD2) is a novel gene related to CRC. Previous studies have suggested that RSAD2 participates in tumor progression in breast cancer, ovarian cancer, and pancreatic adenocarcinoma [16-18]. RSAD2-expressing mature dendritic cells has anticancer response [19]. However, its role in CRC has not been reported. Here, we confirmed that RSAD2 could influence the prognosis and the TME of patients with CRC. In addition, alterations in RSAD2 expression affected the level of pyroptosis. In summary, RSAD2 could serve as a new therapeutic target and potential immune therapeutic and prognostic biomarker for CRC.

Materials and methods

Datasets acquisition

The expression profile and clinical information of 279 CRC samples were downloaded from The Cancer Genome Atlas-colon adenocarcinoma (TCGA-COAD) (http://xena.ucsc.edu) [20]. The transcriptome RNA-seq data and clinical information of CRC patients in the GSE17-536, GSE32323, GSE39582, GSE44076, and GSE9348 datasets were obtained from Gene Expression Omnibus (GEO) (http://www.ncbi.nlm.nih.gov/geo). The TCGA-COAD dataset consisting of 279 CRC samples was used as the training cohort to study the role of RSAD2 in CRC prognosis prediction. Raw data were normalized using the R software package.

Single sample gene set enrichment analysis

The R package "GSVA" was used to conduct single-sample gene set enrichment analysis (ssGSEA). Enrichment of tumor-related hallmarks in TCGA database was performed using ssGSEA. Gene sets of tumor-related hallmarks were downloaded from the MSigDB database (http://www.gsea-msigdb.org).

Weighted gene co-expression networks analysis

The transcriptome profiles of genes were extracted from differential gene expression in TCGA to perform Weighted Gene Co-expression Network Analysis (WGCNA). Sample clustering of pyroptosis trait-related modules was conducted using the R package "WGCNA". A soft-thresholding power of 7, minimal module size of 30, and an abline of 0.25 were set to select key modules. Module eigengene (ME) was regarded as the main principal constituent of a defined gene module. The relationship between ME and pyroptosis was computed to identify modules with a p-value < 0.05.

Identification of hub genes

R package "GEOquery" and "limma" were utilized to compare the expression levels of RSAD2 between normal and CRC tissues. Probe sets lacking clear gene symbols or representing multiple genes were either averaged or excluded. Genes with log fold change (FC) ≥ 1 and adjusted P < 0.05 were defined as differentially expressed genes (DEGs). Hub genes were obtained by intersecting pyroptosis-related genes with DEGs using an online Venn diagram tool (http://bioinformatics.psb.ugent.be).

Protein-protein interaction network and hub gene definition

The screened genes in the protein-protein interaction (PPI) network were identified using a search tool (STRING 11.5; http://cn.string-db.org) [21, 22]. Cytoscape 3.7.3 was used to visualize the networks of genes [23]. The top 24 hub genes with the highest degree were identified using cytohubba, a Cytoscape plugin.

Analysis of the functional pathways of hub genes

Kyoto Encyclopedia of Genes and Genomes (KEGG) (http://www.genome.jp/kegg/) [24] and Gene Ontology (GO) (http://www.geneontology.org/) [25] enrichment analyses were conducted to analyze the pathways and biological functions related to the top 24 hub genes.

The DAVID website (https://david.ncifcrf.gov/) was used for KEGG and GO (including cellular component, biological process, and molecular function) pathway analyses. The data was considered statistically significant with a p-value < 0.05.

Establishment of nomogram for CRC prognosis prediction

A nomogram was established by combining the expression level of RSAD2 and independent clinical characteristics using the R packages "survival" and "rms". The nomogram was aimed at estimating the 1-, 3-, and 5-year survival rates. A calibration curve was used to evaluate model performance.

Immune and stromal cells infiltration

To clarify the complex TME, the cellular composition of stromal and immune cells in each sample was evaluated in TCGA using xCell. The stromal and immune cell scores were calculated for each sample. The CIBERSORTx online website was used to analyze the components of the 22 immune cells in each sample. The absolute levels of the 10 immune cell populations were evaluated using the R package "MCPcount".

Gene set enrichment analysis (GSEA)

The functions of pyroptosis-related genes were investigated using GSEA. Chip expression data and sample information were obtained separately from the training and validation cohorts. Further study was performed using GSEA software. False discovery rate (FDR) < 0.25 and P < 0.05 were considered significant.

Animals study and ethics statement

All animal studies were reported in accordance with ARRIVE guidelines 2.0. All animal procedures also approved by China Three Gorges University Laboratory Animal Management Committee with ethic code number of 202205010D. C57BL/6J mice (7 weeks old, male) were fed individually in specific pathogen-free cages with a 12 h light/12 h dark cycle under free access to water and food.

Patients and volunteers

Blood from the CRC patients and healthy volunteers were obtained from Yichang Central People's Hospital of China. The study was approved by the Ethics Committee of the Yichang Central People's Hospital and followed the declaration of Helsinki with ethic code number: 2021-155-01.

Cell culture

The mice CRC cell line MC38, which purchased from cell bank of Wuhan University, was cultured in Dulbecco's modified Eagle's medium (DMEM) supplemented with 1% antibiotic-antimycotic solution and Zelanian-certified 10% fetal bovine serum (FBS). Cells were cultured in a humidified incubator with 5% CO_2 at 37°C.

Construction of CRC-bearing mice

PBS was utilized to dissolve the MC38 cells into a cell suspension with a density of approximately 6×10^5 cells/ml. The mice were randomly divided into two groups: the control group and the tumor group. The tumor cells were inoculated at the center of the lower back. The entire modeling period lasted for three weeks. It is important to note that the mice were provided with adequate diet and drinking water throughout the CRC modeling period. To anesthetize the mice, intraperitoneal injection of pentobarbital sodium at a dosage of 45 mg/kg was administered. The lower back skin was then disinfected with 75% alcohol. Next, a 1 ml syringe was used to inhale 200 µl of cell suspension. The needle was inserted at a 30° angle into the back and pushed 1 cm subcutaneously. The cell suspension was then slowly injected and the needle was quickly removed once an elliptical bulge appeared on the skin at the injection site. Finally, control mice were injected with 200 µl of PBS in the same manner as the experimental group. Following inoculation, all mice were individually housed and any mice with tumor ulceration were excluded from the study. All mice were sacrificed by cervical dislocation under isoflurane anesthesia.

Knockdown of RSAD2

The DNA sequence encoding small interfering RNA (siRNA) specific for RSAD2 was as follows: forward oligo: 5'-GCUUCAACGUGGACGAAGATT-3'; reverse oligo: 5'-UCUUCGUCCACGUUGAAGCTT-3'. Transfection of RSAD2 siRNA and control siRNA was performed using Lipofectamine 2000 reagent (Invitrogen, Waltham, MA, USA), following the manufacturer's instructions. The knockdown efficiency of

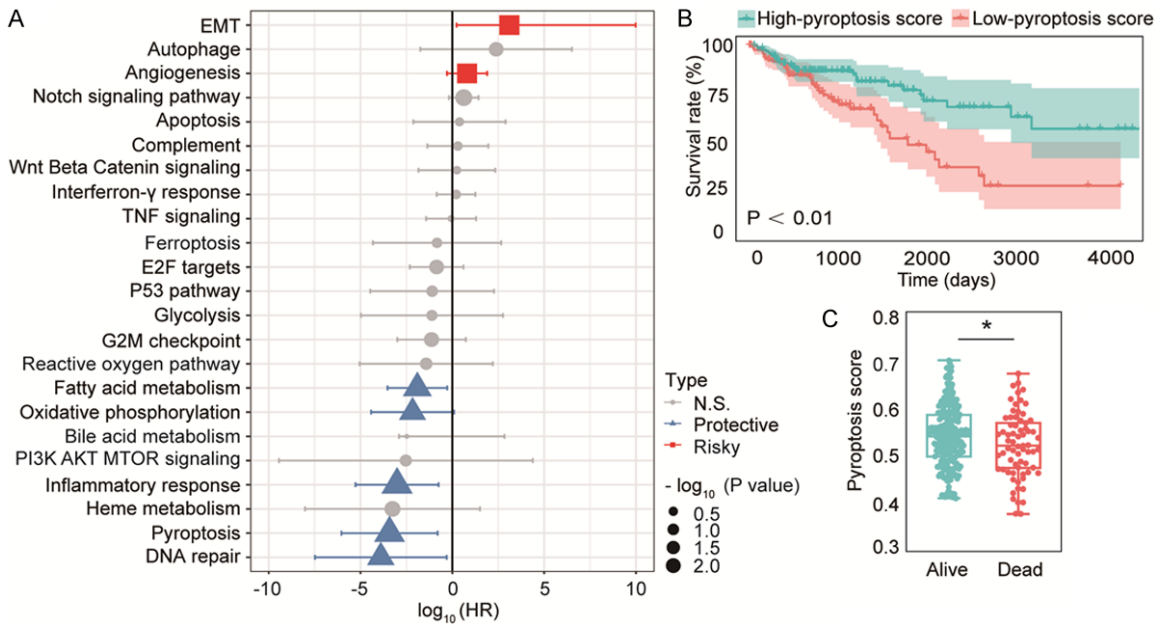

Figure 1. Pyroptosis-related pathways and CRC overall survival (OS). A. Hazard ratio (HR) of 23 cancer pathways for prognosis in the forest plot. B. Kaplan-Meier curve for samples with low pyroptosis score and high pyroptosis score. C. Differences in pyroptosis scores between dead and alive patients.

RASD2 siRNA was estimated by real-time quantitative reverse transcription PCR (RT-qPCR).

RT-qPCR

Total RNA was extracted from cells, tissues, and blood using TRIzol reagent and then reverse-transcribed into cDNA using PrimeScript RT Master Mix. The sequences of these primers are as follows: RSAD2: 5'-CAGTGATTCTCAGGCCGAATA-3' (F), 5'-GGCGAGTACAGACTCACAAA-3' (R); IL-1β: 5'-CACCTCTCAA GCAGAGCACAG-3' (F), 5'-GGGTTCCATGGTGAAGTCAAC-3' (R); IL-6: 5'-GCTACAGCACAAAGCACCTG-3' (F), 5'-TGGAAGATGGTGATGGGATTT-3' (R); TNF-α: 5'-GGCAGCCTTGTCCCTTGAAGAG-3' (F), 5'-GTAGCCCACGTCGT AGCAAACC-3' (R); GSDMD: 5'-CCAACATCTCAGGGCCCCAT-3' (F), 5'-TGGCAAGTTTCTGCCCTGGA-3' (R); GAPDH: 5'-CTGGGCTACACTGAGCAC C-3' (F), 5'-AAGTGGTCGTTGAGGGCAATG-3' (R). The expression of the above targets was quantified using the $2^{-\Delta\Delta Ct}$ method [26], while GAPDH served as an internal control.

Statistical analysis

R and RStudio software were used to analyze the data. To ascertain the hazard ratio (HR) of the forest plots, univariate Cox or multivariate Cox regression analyses were conducted. Survival probability analysis was performed using Kaplan-Meier curves. The differences between the two groups were evaluated using the Wilcoxon test. Statistical significance is defined as follows: $*P < 0.05$, $**P < 0.01$, and $***P < 0.001$.

Results

Pyroptosis considered as an important protective factor related to CRC prognosis

A brief flowchart of this research is shown in Figure S1. RNA-sequencing data from 279 CRC samples were obtained from TCGA dataset using ssGSEA. Cox regression analysis was used to estimate the association between CRC prognosis and various cancer pathways. DNA repair (HR: 1.274×10^{-4}; 95% CI: 3.3×10^{-8}-4.914×10^{-1}; $P < 0.05$), pyroptosis (HR: 3.796×10^{-4}; 95% CI: 9.11×10^{-7}-1.582×10^{-1}; $P < 0.05$) and inflammatory response (HR: 9.77×10^{-4}; 95% CI: 5.34×10^{-6}-1.79×10^{-1}; $P < 0.05$) were closely associated with longer overall survival (OS) in CRC (**Figure 1A**). Meanwhile, DNA repair (HR: 8.8×10^{-5}; 95% CI: 1.3×10^{-7}-5.96×10^{-2}; $P < 0.05$), oxidative phosphorylation (HR: 1.92×10^{-3}; 95% CI: 1.42×10^{-7}-2.59×10^{-1}; $P < 0.05$) and pyroptosis (HR: 3.54×10^{-3}; 95% CI: 1.98×10^{-5}-6.33×10^{-1}; $P < 0.05$) were closely related to longer OS of CRC (Figure S2A).

Overall, pyroptosis was the most important protective factor associated with longer OS. The X-title program was used to select the cutoff to divide CRC patients into low and high pyroptosis score groups. Compared to low pyroptosis scores, high pyroptosis scores were associated with longer OS (**Figures 1B**, S2B). Meanwhile, the pyroptosis score in deceased patients was significantly lower than that in living patients (**Figures 1C**, S2C). These results demonstrate that pyroptosis is a significant protective factor associated with CRC prognosis.

Selection of pyroptosis-related genes in CRC

Co-expression patterns between pyroptosis scores and whole-transcriptome profiling data were compared using WGCNA (**Figure 2A**). A soft-thresholding power of 7 was chosen for building the scale-free network (**Figure 2B**, **2C**) and 0.2 was identified as the threshold for clustering of modules (Figure S3A). Twelve modules were identified (**Figure 2D**, **2E**). The pink, blue, cyan, grey60, midnight blue, and purple modules strongly associated with pyroptosis were chosen to screen PRGs (**Figures 2F**, **2G**, S3B-E).

Analysis of the functional characteristics of common DEGs

To search for DEGs in CRC, the GSE44076 dataset, which contains information on 98 CRC samples and 98 normal control samples, was obtained from the GEO database; there were 1612 DEGs identified (693 upregulated and 909 downregulated in the CRC specimens) (**Figure 3A**). In this study, 1612 DEGs with 1412 PRGs from the WGCNA modules were screened, yielding 288 potential hub genes (**Figure 3B**). The heatmaps of the top 80 hub genes with the highest *p*-values are shown in Figure S4. The top 24 hub genes with the highest degrees were identified in the network (**Figure 3C**). Correlation between pyroptosis and the top 24 hub genes was calculated using the "Corrplot" R package (**Figure 3D**). GO and KEGG pathway enrichment analyses were performed to analyze the biological functions of the top 24 hub genes. GO analysis of the top 24 hub genes was mainly enriched in inflammatory response, extracellular space, and chemokine activity (**Figure 3E**; **Table 1**). KEGG pathway analysis of the top 24 hub genes confirmed that the most significant pathways were cytokine-cytokine receptor interaction, chemokine signaling, and TNF signaling (**Figure 3F**; **Table 2**). Taken together, these results indicate that CRC progression is closely associated with the immune response.

Associations between top 24 hub genes, including RSAD2, and survival analysis

Gene expression levels were examined using GSE44076. CCL5, CXCL13, FOS, IFIT1, ISG15, MX1, RSAD2, and TLR3 were significantly downregulated, while the others were upregulated (**Figure 4**). Kaplan-Meier analysis was performed to investigate the relationship between hub genes and CRC prognosis. High expression of ISG15, MX1, and RSAD2 predicted poor OS, and individuals with higher expression of CXCL2, CXCL8, CXCL13, IL-1α, and IL-1β had better clinical outcomes in TCGA database (**Figure 5A-H**). Additionally, there was no significant correlation between CRC prognosis and CCL3, CCL5, CXCL1, CXCL5, CXCL9, CXCL10, CXCL11, FCGR3A, FOS, GZMB, IFIT1, MMP1, MMP3, MMP9, SPP1, or TLR3 (Figure S5). Among these hub genes, we discovered that RSAD2 is a novel gene associated with CRC and may be related to the progression and prognosis of CRC. In addition, high expression of RSAD2 was associated with worse DSS and PFI than low expression in TCGA cohorts (**Figure 5I**, **5J**). To demonstrate the reliability of RSAD2, two additional independent datasets were used for validation. The link between high RSAD2 expression and shorter OS was also confirmed in GSE17536 and GSE39582 (**Figure 5K**, **5L**). In summary, these results indicate that RSAD2 may be a novel candidate target for CRC prognosis.

Prognostic role of RSAD2 in CRC

To verify the role of RSAD2 in CRC prognosis, the correlation between RSAD2 mRNA levels and various clinicopathological characteristics was analyzed in the TCGA dataset. RSAD2 was noticeably increased in the advanced clinical stages, pathologic T3 and T4, lymphatic invasion, and progression subtypes compared with the primary clinical stage, pathologic T1 and T2, non-lymphatic invasion, and progression subtypes (**Figure 6A-D**). Univariate and multivariate Cox regression analyses were performed to determine the general prognostic value. The results demonstrated that high

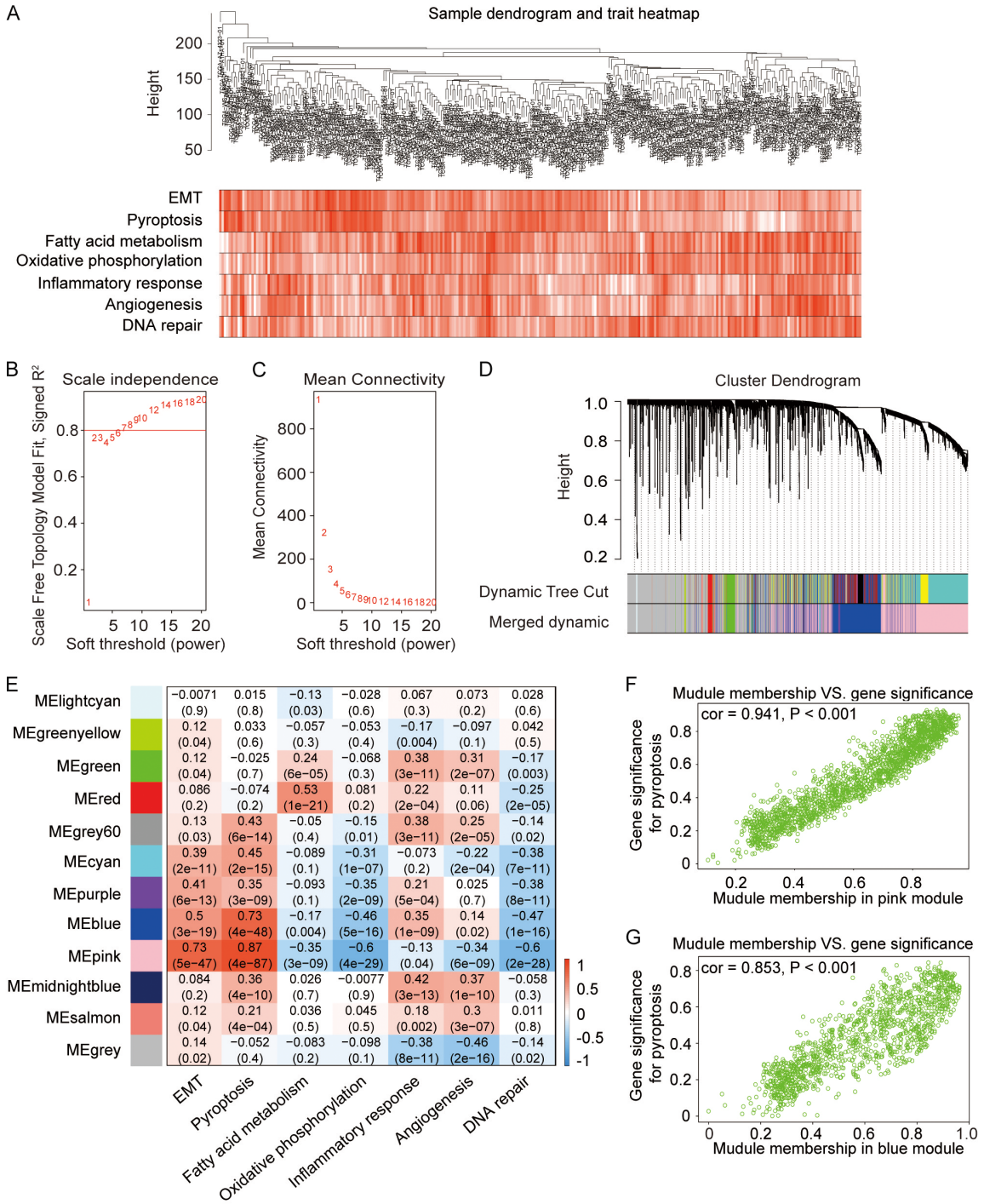

Figure 2. Selection of pyroptosis-related genes of CRC. (A) Clustering dendrogram of 279 samples from the TCGA using WGCNA. Calculation of the scale-free index (B) and the mean connectivity (C) in different soft-threshold powers (β). (D) Clustered dendrogram for differentially expressed genes. (E) Heatmap of the relevance between the modules and cancer pathways. Relevance between pyroptosis and pink module (F), blue module (G).

RSAD2 expression was an independent risk factor for OS of patients with CRC (for univariate analysis, combined HR = 2.078, 95% CI = 1.139-3.674, P = 0.013; for multivariate analysis, combined HR = 1.892, 95% CI = 0.998-3.586, P = 0.042) (**Figure 6E**). To better predict the prognosis of CRC patients, a nomogram was developed by integrating RSAD2 levels and independent clinicopathological characteristics (age, sex, pathologic T, N, and M) of the

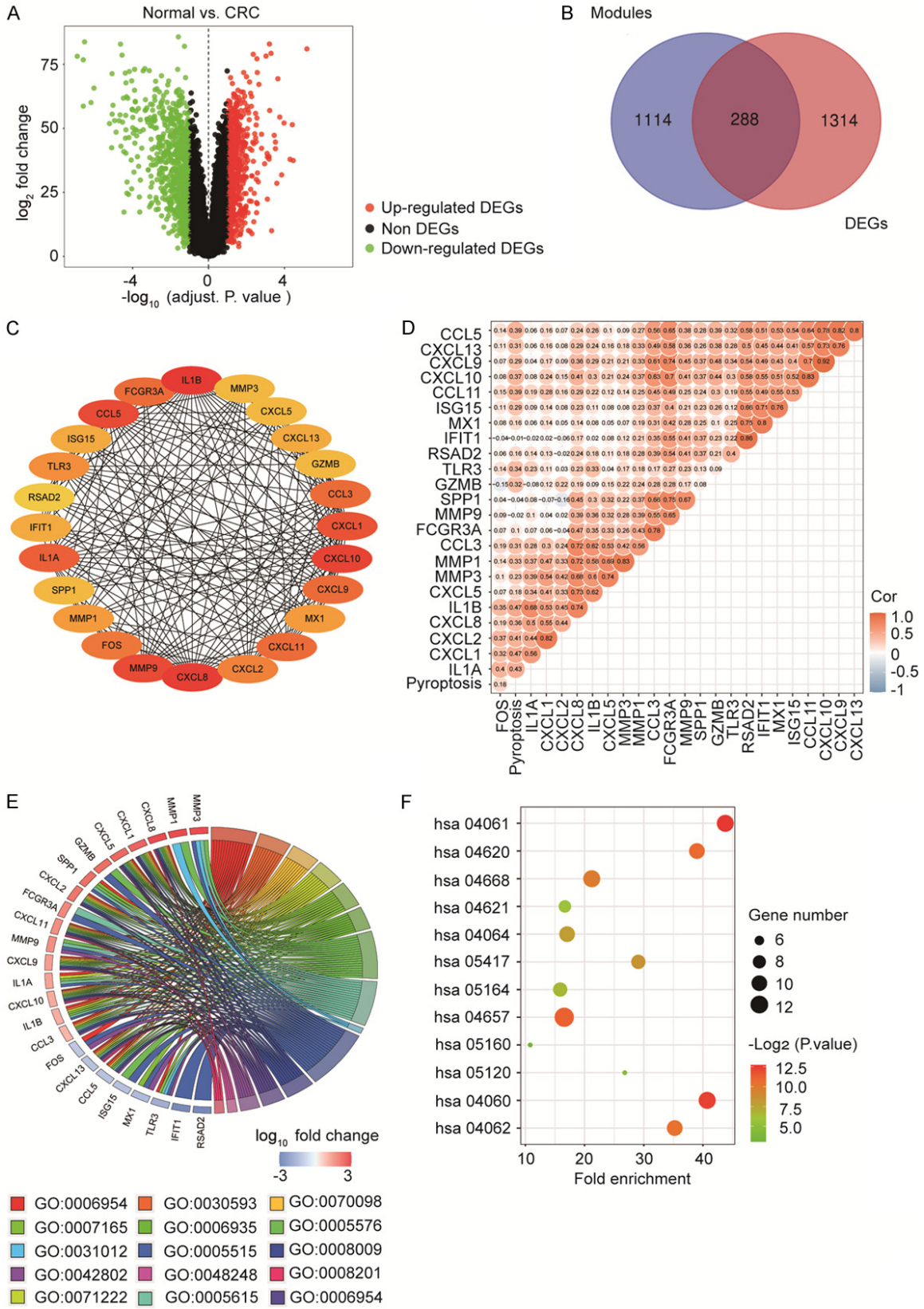

Figure 3. Relevance and pathway analysis of pyroptosis-related genes. (A) Differentially expressed genes (DEGs) based on GSE44076 data in the volcano plot. (B) Intersection of DEGs and selected genes from WGCNA in the venn plot. (C) The protein-protein interaction network of top 24 hub genes. (D) The relevance between top 24 hub genes and pyroptosis. GO enrichment analysis (E) and KEGG enrichment analysis (F) for top 24 hub genes.

Table 1. Enrichment and functional of GO analyses for top 24 hub genes

Term	Name	Count	*P* value	Genes
GO:0006954	Inflammatory response A	15	1.8E-18	CXCL9, CXCL8, CXCL1, FOS, CXCL13, CXCL2, CXCL5, IL1A, CXCL10, CXCL11, IL1B, CCL5, SPP1, CCL3, TLR3
GO:0030593	Neutrophil chemotaxis	11	1.1E-18	CXCL10, CXCL11, CXCL9, CXCL8, CCL5, IL1B, CCL3, CXCL1, CXCL13, CXCL2, CXCL5
GO:0070098	Chemokine-mediated pathway	10	5.3E-17	CXCL10, CXCL11, CXCL9, CXCL8, CCL5, CCL3, CXCL1, CXCL13, CXCL2, CXCL5
GO:0071222	Cellular response lipopolysaccharide	10	5.3E-13	IL1A, CXCL10, CXCL11, CXCL9, CXCL8, IL1B, CXCL1, CXCL13, CXCL2, CXCL5
GO:0007165	Signal transduction	10	5.6E-6	CXCL10, CXCL11, CXCL9, CXCL8, IL1B, MX1, SPP1, CXCL1, CXCL5, TLR3
GO:0006935	Chemotaxis	9	1.0E-12	CXCL10, CXCL11, CXCL9, CXCL8, CCL5, CCL3, CXCL1, CXCL2, CXCL5
GO:0005576	Extracellular region	18	1.2E-12	CXCL9, CXCL8, MMP1, MMP3, GZMB, ISG15, CXCL1, CXCL2, MMP9
GO:0005615	Extracellular space	17	4.9E-12	MMP1, MMP3, TLR3
GO:0031012	Extracellular matrix	3	3.4E-2	CXCL9, CXCL8, RSAD2, MX1, MMP3, GZMB, ISG15, CXCL1, FOS, IFIT1
GO:0005515	Protein binding	22	6.8E-3	CXCL10, CXCL11, CXCL9, CXCL8, CCL5, CCL3, CXCL1, CXCL13
GO:0008009	Chemokine activity	10	2.5E-18	CXCL10, CXCL11, CXCL9, CXCL8, CXCL1, CXCL13, CXCL2
GO:0045236	CXCR chemokine receptor binding	8	9.7E-18	CCL5, MX1, CCL3, FOS, MMP9, CXCL5, TLR3
GO:0042802	Identical protein binding	7	1.4E-2	GZMB, ISG15, CXCL1, CXCL13, CXCL2, MMP9
GO:0048248	CXCR3 chemokine receptor binding	4	1.6E-8	CXCL10, CXCL11, CXCL9, CXCL13
GO:0008201	Heparin binding	4	1.2E-3	CXCL10, CXCL11, CXCL8, CXCL13

Table 2. Enrichment and functional of KEGG analyses for top 24 hub genes

Term	Name	Count	*P* value	Genes
hsa04061	Viral protein interaction with cytokine	10	1.9E-13	IL1A, CXCL8, MMP1, CCL5, IL1B, CCL3, CXCL1, FOS, CXCL2, CXCL5
hsa04060	Cytokine-receptor interaction	10	3.7E-13	CXCL10, CXCL11, CXCL9, CXCL8, CCL5, CCL3, CXCL1, CXCL13, CXCL2, CXCL5
hsa04657	IL-17 signaling pathway	12	6.9E-12	IL1A, CXCL10, CXCL11, CXCL9, CXCL8, CCL5, IL1B, CCL3, CXCL1, CXCL13, CXCL2, CXCL5
hsa04620	Toll-like receptor signaling pathway	9	1.6E-11	CXCL10, CXCL8, MMP1, IL1B, CXCL1, FOS, CXCL2, MMP9, CXCL5
hsa04062	Chemokine signaling pathway	9	3.6E-11	CXCL10, CXCL11, CXCL9, CXCL8, CCL5, IL1B, CCL3, FOS, TLR3
hsa04668	TNF signaling pathway	10	1.4E-10	CXCL10, CXCL11, CXCL9, CXCL8, CCL5, CCL3, CXCL1, CXCL13, CXCL2
hsa05417	Lipid and atherosclerosis	8	3.4E-9	CXCL10, CCL5, IL1B, CXCL1, FOS, CXCL2, MMP9, CXCL5
hsa04064	NF-kappa B signaling pathway	9	1.2E-8	CXCL8, MMP1, CCL5, IL1B, CCL3, CXCL1, FOS, CXCL2, MMP9
hsa04621	NOD-like receptor signaling pathway	7	1.7E-6	IL1A, CXCL10, CXCL8, CCL5, IL1B, MX1, TLR3
hsa05120	Epithelial cell signaling in Helicobacter	5	2.4E-5	IL1A, CXCL8, IL1B, FOS, CXCL5
hsa05164	Influenza A	8	2.9E-7	IL1A, CXCL10, CXCL8, RSAD2, CCL5, IL1B, MX1, TLR3
hsa05160	Hepatitis C	5	8.9E-4	CXCL10, RSAD2, MX1, IFIT1, TLR3

patients (**Figure 6F**). The areas under the receiver operator characteristic (ROC) curve for 1-, 3-, and 5-year OS of the nomogram were 0.752, 0.865, and 0.759, respectively (**Figure 6G**). The calibration plot of the agreement revealed high agreement between the observed outcomes and predicted 1-, 3-, and 5-year survival of the nomogram (**Figure 6H-J**). The prognostic role of RSAD2 was verified using the GSE39582 dataset (Figure S6). In general, RSAD2 can be identified as an independent prognostic factor in patients with CRC.

Mechanism of pyroptosis in TME of CRC

Relevance analysis of hypoxia-related gene signature (HGS) and stromal and immune cells was performed to elucidate the potential role of pyroptosis in the TME. The results showed that pyroptosis was negatively correlated with the stromal score and positively correlated with the immune score, implying its possible role mediated by stromal and immune cells in tumor progression (**Figure 7A**, **7B**). A correlation matrix between RSAD2 and immune cells demonstrated that M2 macrophages and $CD4^+$ naive T-cells were positively related to RSAD2, whereas plasmacytoid DCs (pDCs), mast cells, M1 macrophages, and B-cells were negatively related to RSAD2 (**Figure 7C**). The former group was associated with shorter OS, while the latter group was linked with better OS (**Figure 7D**). Additionally, 13 immune cells were found to be related to pyroptosis in CRC. Among them,

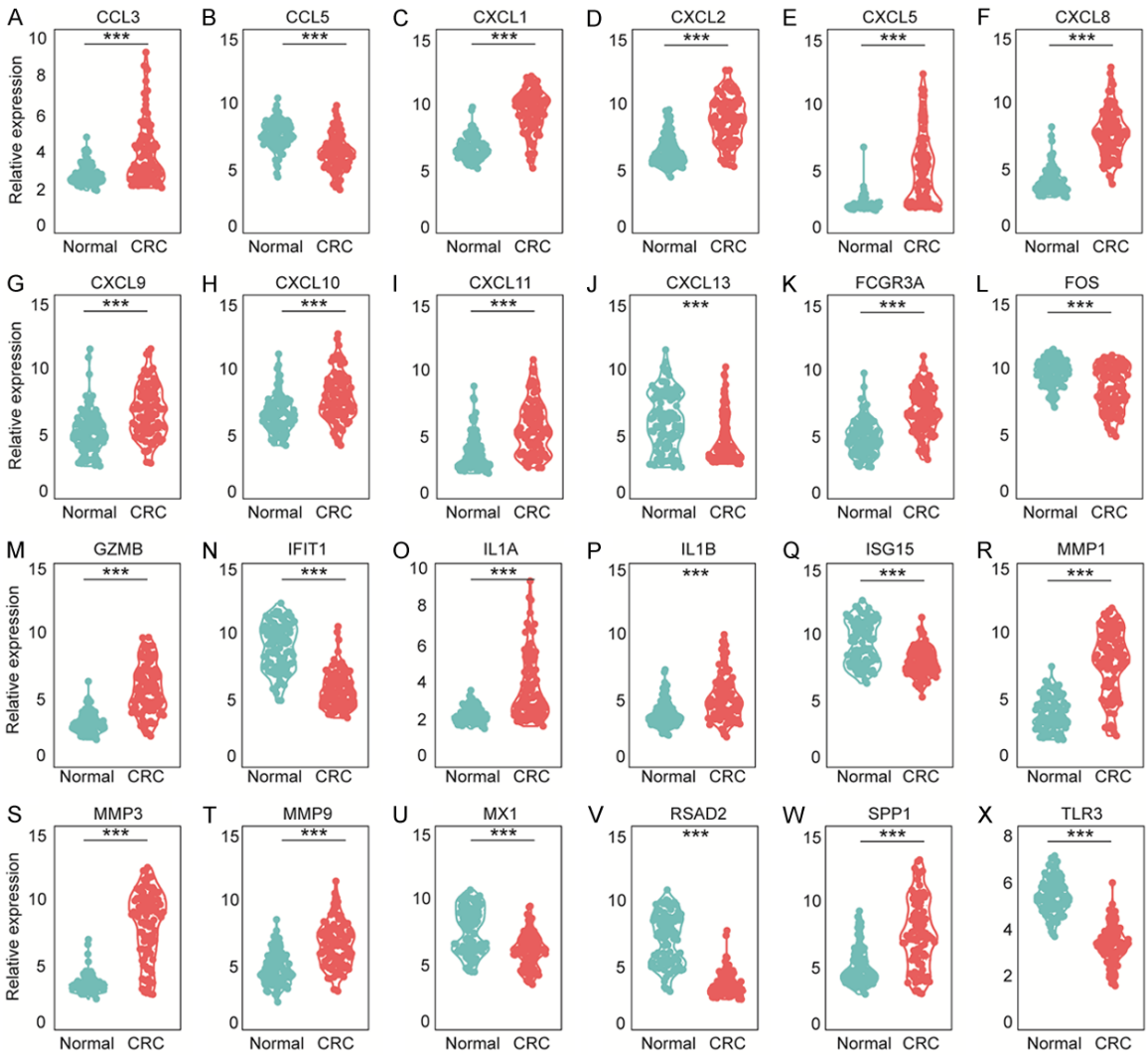

Figure 4. Comparison of the expression levels of pyroptosis-related genes in normal and CRC samples. A-X. The expression difference of hub genes between normal tissues and colorectal cancer tissues.

pDCs, B-cells, pro B-cells, $CD8^+$ T-cells, M1 macrophages, mast cells, NK cells, and Th1 cells were significantly higher in the RSAD2-low group, whereas DCs, $CD4^+$ naive T-cells, M2 macrophages, and plasma cells were significantly higher in the RSAD2-high group (**Figures 7E**, S7). To evaluate the immune response between the two groups, the expression of immune checkpoint-related genes such as PD1 and PDL1 as well as immune active genes, such as OX40, CD40, and CD86, were explored. All sets of genes were upregulated in the RSAD2-low group using the Wilcoxon test (**Figure 7F**). Overall, pyroptosis may be involved in changes in the TME and immunotherapy of CRC.

Expression level of RSAD2 and its correlation with pyroptosis

Two additional independent datasets (GSE-32323 and GSE9348) were used to confirm the stability of the RSAD2. Compared to normal samples, the expression of RSAD2 was significantly decreased in CRC patients (**Figure 8A**, **8B**). Transcriptome expression results from CRC and paired normal samples were used to identify potential molecules for CRC diagnosis; the diagnostic accuracies of the RSAD2 were 0.824 and 0.910, respectively (**Figure 8C**, **8D**). To verify the above findings, blood samples from nine CRC patients and nine normal volunteers were analyzed using RT-qPCR. The results

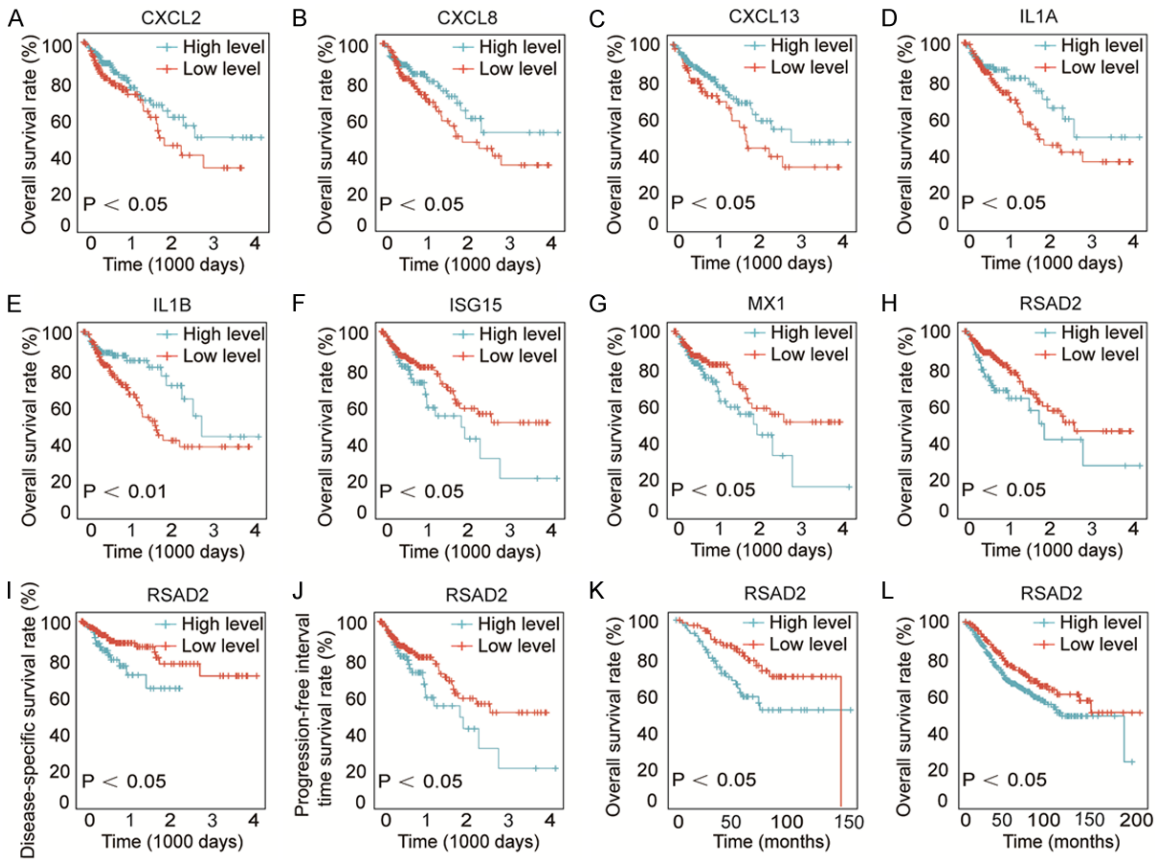

Figure 5. Kaplan-Meier survival curves of CRC samples with high (blue lines) and low (red lines) expression of hub genes. Kaplan-Meier OS curves for patients with different levels of CXCL2 (A), CXCL8 (B), CXCL13 (C), IL-1A (D), IL-1B (E), ISG15 (F), MX1 (G) and RSAD2 (H) in the TCGA. Kaplan-Meier DSS curves (I) and PFI curves (J) for RSAD2-low and RSAD2-high groups in the TCGA. Kaplan-Meier OS curves for RSAD2-low and RSAD2-high groups in the GSE17536 (K) and GSE39582 (L).

showed that RSAD2 mRNA level was lower in CRC patients (**Figure 8E**), and the same results were observed in the tissues and blood of control mice and CRC-bearing mice (**Figure 8F**, **8G**). The expression of RSAD2 gene in the RSAD2-low group was found to be related to pyroptosis induction by GSEA (**Figures 8H**, S8). To investigate the effect of RSAD2 on pyroptosis, siRNA was used to knockdown RSAD2 in MC38 cells (**Figure 8I**). Compared with MC38 cells, the mRNA expression levels of GSDMD, TNF-α, IL-1β, and IL-6 were increased in siRSAD2 MC38 cells by RT-qPCR (**Figure 8J-M**). Therefore, RSAD2 may reduce pyroptosis.

Discussion

In recent years, an increasing number of people have been diagnosed with cancer, and CRC remains the second leading cause of cancer-related death. However, the prognostic value of CRC remains poor. The development of genomic data is changing the situation by exploiting to screen the targets of treatment. Consequently, the search for efficient prognostic markers is necessary to improve clinical outcomes in patients with CRC.

Pyroptosis is a new form of programmed cell death (PCD) that is involved in the development and progression of various tumors [27, 28]. However, the relationship between pyroptosis and cancer remains controversial. Pyroptosis can inhibit tumor development [29, 30]. A previous study showed that pyroptosis of tumor cells induces inflammation and triggers a robust antitumor immune response [31]. In contrast, pyroptosis promotes tumor growth [30, 32]. As a pro-inflammatory mediator, pyroptosis offers a suitable microenvironment for tumor cell growth and indirectly facilitates tumor development. In the present study, we revealed that

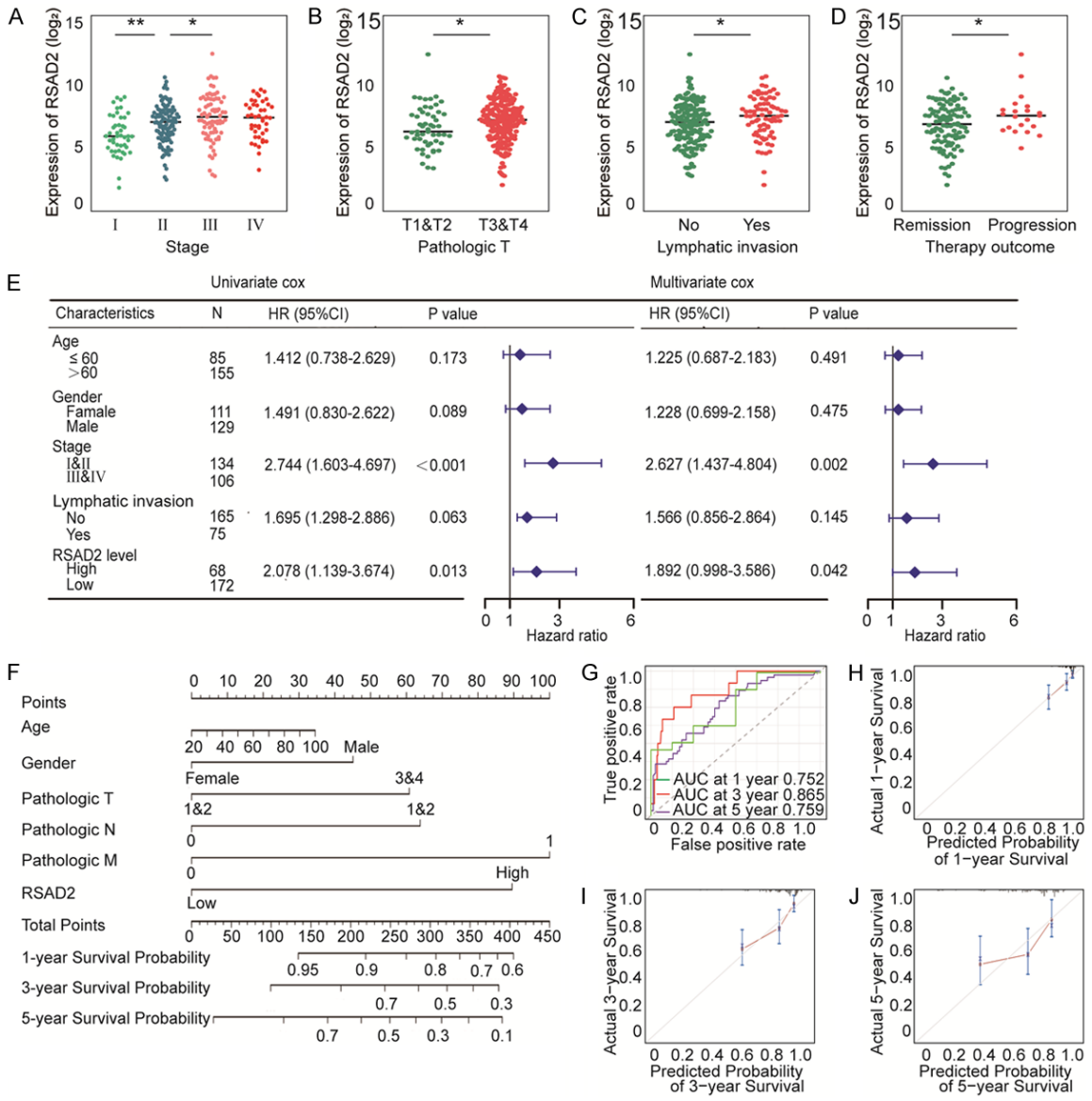

Figure 6. Identification of RSAD2 as a key gene and an independent prognostic factor of CRC. A-D. Analysis of correlation between RSAD2 mRNA expression and different subtypes of CRC tissues from TCGA database. E. Univariate and multivariate Cox regression analyses of RSAD2, age, gender, tumor stage and lymphatic invasion. F. Prediction of CRC patient prognosis by the nomogram established based on multivariate Cox regression analysis. G. Time-dependent ROC curves of the nomogram in predicting 1-, 3- and 5-year OS. H-J. Comparison between actual and nomogram-predicted 1-, 3- and 5-year OS in the calibration plot.

pyroptosis is a protective factor in CRC and influences CRC prognosis. Many researchers have argued that the bidirectional effect of pyroptosis on tumors may depend on the tumor type, host inflammatory status, and genetic background [30].

WGCNA was used to identify the pyroptosis-related genes where 288 overlapping genes were identified through 1114 genes from pyroptosis-related gene modules and 1314 genes from DEGs. We selected the top 24 genes for further investigation, most of which were inflammatory factors and chemokines. Various studies have reported a close correlation between CXC chemokine expression and prognosis of patients with CRC. Studies have demonstrated that CXCL1 and CXCL11 regulate progression and invasion and accelerate anti-tumor immunity in CRC [33, 34]. Furthermore,

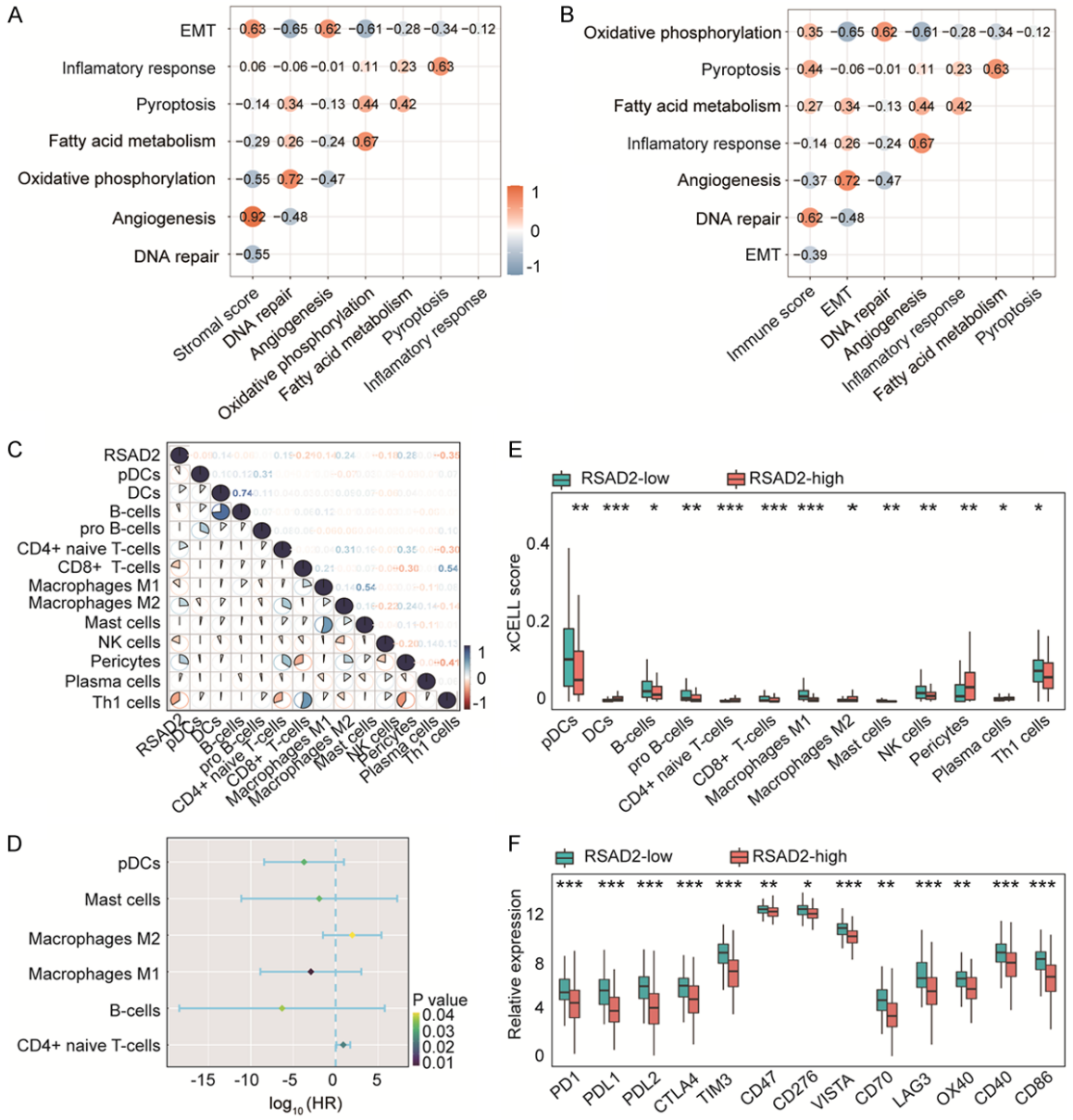

Figure 7. Immunological changes of RSAD2 in CRC microenvironment. A, B. Spearman relevance analysis between pyroptosis and stromal cells, immune cells and infiltration. C. The correlation between RSAD2 and various immune cells. D. Hazard ratio (HR) of various prognostic immune cells in the forest plot. E. The infiltration pattern of 13 immune cells in RSAD2-low and RSAD2-high groups. F. Expression level of immune checkpoint-related genes and immune active genes in RSAD2-low and RSAD2-high groups.

high expression levels of CXCL2/3/8/9/10/11/14 are correlated with clinical outcomes of patients with CRC [35], which is consistent with our results. Our study showed that high expression of CXCL2/8/13, IL-1α, and IL-1β was associated with better OS, while low ISG15, MX1, and RSAD2 expression was associated with better OS in CRC patients. Notably, RSAD2 was found to be a novel gene that has not yet been studied in patients with CRC. Previous studies have revealed that RSAD2 facilitates the development and metastasis of uveal melanoma [36] and is associated with immune cell infiltration in patients with pancreatic adenocarcinoma [18]. Other bioinformatic analyses have also shown that RSAD2 is associated with tumor stage, grade, and lymph node metastases, and may be a prognostic candidate for breast cancer [16]. In addition, Gromova et al. reported that RSAD2 is upregulated in gastroin-

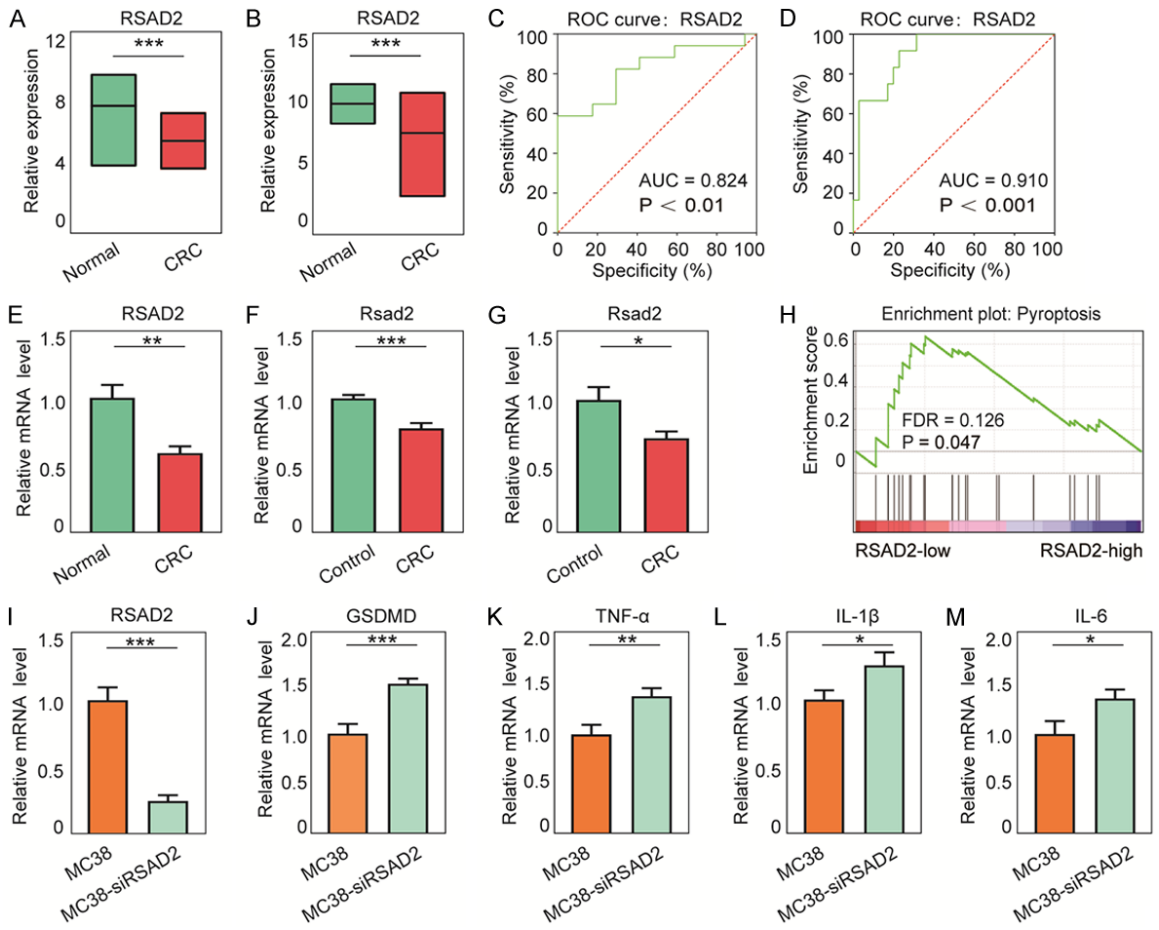

Figure 8. Expression changes of RSAD2 in CRC and its effect on pyroptosis. The expression levels (A, B) and diagnostic accuracy (C, D) of RSAD2 in the GSE32323 and GSE9348. (E) Expression of RSAD2 mRNA level in tissues from normal volunteers and CRC patients (n = 9 per group). (F, G) The expression levels of RSAD2 mRNA in the blood and tissues from control mice and CRC-bearing mice (n = 8 per group). (H) GSEA of pyroptosis pathway in RSAD2-low and RSAD2-high groups. (I-M) Expression of RSAD2, GSDMD, TNF-α, IL-1β and IL-6 genes in MC38 and MC38-siRSAD cell lines (n = 8 per group).

testinal stromal tumors [37]. In the current study, we found that RSAD2 was associated with tumor stage, lymphatic invasion, therapy outcome, and prognosis of CRC; however, more in-depth studies are needed.

Numerous studies have revealed that pyroptosis plays a vital role in inflammatory and immune responses. Pyroptosis can stimulate the innate immune system and inhibit the development of tumor cells by altering the TME. A previous study showed a significantly poor prognosis in colon cancer patients with high stromal components [38], which is consistent with our result showing a negative relationship between pyroptosis and stromal cells. Other infiltrating immune cells also influence pyroptosis in the TME. Wang et al. revealed that pyroptosis in a small proportion of tumor cells was sufficient to effectively regulate the TME, which activated a strong T-cell-mediated antitumor immune response [31]. Zhang et al. also showed that pyroptosis suppresses tumor growth by activating anti-tumor immunity [29]. Our research suggests that RSAD2 is positively correlated with M2 macrophage and $CD4^+$ T-cell infiltration and negatively correlated with pDCs, mast cells, M1 macrophages, and B-cells, indicating potential differences in immune function between the two groups. Moreover, other studies have reported that RSAD2 is necessary for myeloid DC maturation [19]. Although more studies are needed to confirm these findings, RSAD2 may be related to the TME in CRC patients.

In recent years, immune checkpoint inhibitors have become the primary treatment option for

patients with CRC, along with surgery, chemotherapy, and radiotherapy. Studies have shown that pyroptosis is related to immune checkpoints [39]. Our results revealed that the RSAD2-low group expressed more immune checkpoint genes, including PD1, PDL1, PDL2, CTLA4, TIM3, CD47, CD276, VISTA, CD70, and LAG3, in the TME of CRC patients. Other reports have shown that PDL1 inhibitors combined with chemotherapy or radiotherapy kill tumor cells by inducing pyroptosis in tumor cells [39]. In summary, RSAD2 may kill tumor cells by decreasing the expression of immune checkpoint genes.

While a comprehensive analysis of PRGs in CRC patients was conducted and some conclusions from a clinical perspective were obtained in the current study, the role of RSAD2 in prognosis and immunotherapy still needed to be further validated, so additional experiments were performed. GSDMD is a powerful executor of pyroptosis and is associated with immune response [40, 41]. We discovered that the augmentation of GSDMD levels increased the inflammatory response, such as the boost of TNF-α, IL-1β, and IL-6, which is consistent with a previous study, indicating that pyroptosis may participate in the TME by activating the immune response. Furthermore, RSAD2 was sharply decreased in CRC samples *in vivo* and *in vitro*, and RSAD2 deletion also influenced the level of pyroptosis.

In summary, RSAD2, a pyroptosis-related gene, plays an important role in CRC and provides a better treatment strategy for CRC patients. However, some limitations need to be considered in the paper. Firstly, we only used blood samples of CRC patients to verify the role of RSAD2, and large-scale prospective studies and additional in *vivo* and in *vitro* experimental studies need to be performed. Secondly, more in-depth mechanisms regarding the role of RSAD2 in CRC should be systematically elucidated through experimental methods. Taken together, this study indicates that RSAD2 may be as a biomarker to accurately predict the prognosis of CRC patients and expects to be a potential therapeutic target in CRC patients.

Acknowledgements

We would like to thank Editage (www.editage.cn) for English language editing. The study was supported by the National Natural Science Foundation of China (82304470), and the Natural Science Foundation of Hubei Province (2022CFB650).

Informed consent was obtained from all patients included in the study.

Disclosure of conflict of interest

None.

Address correspondence to: Yanyan Wang and Xinhua Xu, The First College of Clinical Medical Science, China Three Gorges University/Yichang Central People's Hospital, No. 183, Yiling Avenue, Wujiagang District, Yichang 443000, Hubei, China. E-mail: wangyy1001@163.com (YYW); 2732774-352@qq.com (XHX)

References

[1] Bray F, Ferlay J, Soerjomataram I, Siegel RL, Torre LA and Jemal A. Global cancer statistics 2018: GLOBOCAN estimates of incidence and mortality worldwide for 36 cancers in 185 countries. CA Cancer J Clin 2018; 68: 394-424.

[2] Siegel RL, Miller KD, Wagle NS and Jemal A. Cancer statistics, 2023. CA Cancer J Clin 2023; 73: 17-48.

[3] Siegel RL, Wagle NS, Cercek A, Smith RA and Jemal A. Colorectal cancer statistics, 2023. CA Cancer J Clin 2023; 73: 233-254.

[4] Wang Y, Gao W, Shi X, Ding J, Liu W, He H, Wang K and Shao F. Chemotherapy drugs induce pyroptosis through caspase-3 cleavage of a gasdermin. Nature 2017; 547: 99-103.

[5] Tan Y, Chen Q, Li X, Zeng Z, Xiong W, Li G, Li X, Yang J, Xiang B and Yi M. Pyroptosis: a new paradigm of cell death for fighting against cancer. J Exp Clin Cancer Res 2021; 40: 153.

[6] Song W, Ren J, Xiang R, Kong C and Fu T. Identification of pyroptosis-related subtypes, the development of a prognosis model, and characterization of tumor microenvironment infiltration in colorectal cancer. Oncoimmunology 2021; 10: 1987636.

[7] Liao P, Huang WH, Cao L, Wang T and Chen LM. Low expression of FOXP2 predicts poor survival and targets caspase-1 to inhibit cell pyroptosis in colorectal cancer. J Cancer 2022; 13: 1181-1192.

[8] Wang J, Kang Y, Li Y, Sun L, Zhang J, Qian S, Luo K, Jiang Y, Sun L and Xu F. Gasdermin D in different subcellular locations predicts diverse progression, immune microenvironment and prognosis in colorectal cancer. J Inflamm Res 2021; 14: 6223-6235.

[9] Rao Z, Zhu Y, Yang P, Chen Z, Xia Y, Qiao C, Liu W, Deng H, Li J, Ning P and Wang Z. Pyroptosis in inflammatory diseases and cancer. Theranostics 2022; 12: 4310-4329.
[10] Tan G, Huang C, Chen J and Zhi F. HMGB1 released from GSDME-mediated pyroptotic epithelial cells participates in the tumorigenesis of colitis-associated colorectal cancer through the ERK1/2 pathway. J Hematol Oncol 2020; 13: 149.
[11] Sborgi L, Ruhl S, Mulvihill E, Pipercevic J, Heilig R, Stahlberg H, Farady CJ, Muller DJ, Broz P and Hiller S. GSDMD membrane pore formation constitutes the mechanism of pyroptotic cell death. EMBO J 2016; 35: 1766-1778.
[12] Liu X, Zhang Z, Ruan J, Pan Y, Magupalli VG, Wu H and Lieberman J. Inflammasome-activated gasdermin D causes pyroptosis by forming membrane pores. Nature 2016; 535: 153-158.
[13] Erkes DA, Cai W, Sanchez IM, Purwin TJ, Rogers C, Field CO, Berger AC, Hartsough EJ, Rodeck U, Alnemri ES and Aplin AE. Mutant BRAF and MEK inhibitors regulate the tumor immune microenvironment via pyroptosis. Cancer Discov 2020; 10: 254-269.
[14] Wu J, Zhu Y, Luo M and Li L. Comprehensive analysis of pyroptosis-related genes and tumor microenvironment infiltration characterization in breast cancer. Front Immunol 2021; 12: 748221.
[15] Du T, Gao J, Li P, Wang Y, Qi Q, Liu X, Li J, Wang C and Du L. Pyroptosis, metabolism, and tumor immune microenvironment. Clin Transl Med 2021; 11: e492.
[16] Tang J, Yang Q, Cui Q, Zhang D, Kong D, Liao X, Ren J, Gong Y and Wu G. Weighted gene correlation network analysis identifies RSAD2, HERC5, and CCL8 as prognostic candidates for breast cancer. J Cell Physiol 2020; 235: 394-407.
[17] Kurokawa C, Iankov ID and Galanis E. A key anti-viral protein, RSAD2/VIPERIN, restricts the release of measles virus from infected cells. Virus Res 2019; 263: 145-150.
[18] Zuo D, Chen Y, Zhang X, Wang Z, Jiang W, Tang F, Cheng R, Sun Y, Sun L, Ren L and Liu R. Identification of hub genes and their novel diagnostic and prognostic significance in pancreatic adenocarcinoma. Cancer Biol Med 2021; 19: 1029-46.
[19] Jang JS, Lee JH, Jung NC, Choi SY, Park SY, Yoo JY, Song JY, Seo HG, Lee HS and Lim DS. Rsad2 is necessary for mouse dendritic cell maturation via the IRF7-mediated signaling pathway. Cell Death Dis 2018; 9: 823.
[20] Hutter C and Zenklusen JC. The Cancer Genome Atlas: creating lasting value beyond its data. Cell 2018; 173: 283-285.
[21] Szklarczyk D, Franceschini A, Wyder S, Forslund K, Heller D, Huerta-Cepas J, Simonovic M, Roth A, Santos A, Tsafou KP, Kuhn M, Bork P, Jensen LJ and von Mering C. STRING v10: protein-protein interaction networks, integrated over the tree of life. Nucleic Acids Res 2015; 43: D447-452.
[22] Szklarczyk D, Morris JH, Cook H, Kuhn M, Wyder S, Simonovic M, Santos A, Doncheva NT, Roth A, Bork P, Jensen LJ and von Mering C. The STRING database in 2017: quality-controlled protein-protein association networks, made broadly accessible. Nucleic Acids Res 2017; 45: D362-D368.
[23] Su G, Morris JH, Demchak B and Bader GD. Biological network exploration with Cytoscape 3. Curr Protoc Bioinformatics 2014; 47: 8.13.11-24.
[24] Kanehisa M and Goto S. KEGG: Kyoto encyclopedia of genes and genomes. Nucleic Acids Res 2000; 28: 27-30.
[25] Davis S and Meltzer PS. GEOquery: a bridge between the Gene Expression Omnibus (GEO) and bioConductor. Bioinformatics 2007; 23: 1846-1847.
[26] Livak KJ and Schmittgen TD. Analysis of relative gene expression data using real-time quantitative PCR and the 2(-Delta Delta C(T)) method. Methods 2001; 25: 402-408.
[27] Yu P, Zhang X, Liu N, Tang L, Peng C and Chen X. Pyroptosis: mechanisms and diseases. Signal Transduct Target Ther 2021; 6: 128.
[28] Fang Y, Tian S, Pan Y, Li W, Wang Q, Tang Y, Yu T, Wu X, Shi Y, Ma P and Shu Y. Pyroptosis: a new frontier in cancer. Biomed Pharmacother 2020; 121: 109595.
[29] Zhang Z, Zhang Y, Xia S, Kong Q, Li S, Liu X, Junqueira C, Meza-Sosa KF, Mok TMY, Ansara J, Sengupta S, Yao Y, Wu H and Lieberman J. Gasdermin E suppresses tumour growth by activating anti-tumour immunity. Nature 2020; 579: 415-420.
[30] Xia X, Wang X, Cheng Z, Qin W, Lei L, Jiang J and Hu J. The role of pyroptosis in cancer: pro-cancer or pro-"host"? Cell Death Dis 2019; 10: 650.
[31] Wang Q, Wang Y, Ding J, Wang C, Zhou X, Gao W, Huang H, Shao F and Liu Z. A bioorthogonal system reveals antitumour immune function of pyroptosis. Nature 2020; 579: 421-426.
[32] Zhou CB and Fang JY. The role of pyroptosis in gastrointestinal cancer and immune responses to intestinal microbial infection. Biochim Biophys Acta Rev Cancer 2019; 1872: 1-10.
[33] Zhuo C, Wu X, Li J, Hu D, Jian J, Chen C, Zheng X and Yang C. Chemokine (C-X-C motif) ligand 1 is associated with tumor progression and poor prognosis in patients with colorectal cancer. Biosci Rep 2018; 38: BSR20180580.

[34] Cao Y, Jiao N, Sun T, Ma Y, Zhang X, Chen H, Hong J and Zhang Y. CXCL11 correlates with antitumor immunity and an improved prognosis in colon cancer. Front Cell Dev Biol 2021; 9: 646252.
[35] Yang X, Wei Y, Sheng F, Xu Y, Liu J, Gao L, Yang J, Sun X, Huang J and Guo Q. Comprehensive analysis of the prognosis and immune infiltration for CXC chemokines in colorectal cancer. Aging (Albany NY) 2021; 13: 17548-17567.
[36] Xie M and Xin C. RASD2 promotes the development and metastasis of uveal melanoma via enhancing glycolysis. Biochem Biophys Res Commun 2022; 610: 92-98.
[37] Gromova P, Ralea S, Lefort A, Libert F, Rubin BP, Erneux C and Vanderwinden JM. Kit K641E oncogene up-regulates Sprouty homolog 4 and trophoblast glycoprotein in interstitial cells of Cajal in a murine model of gastrointestinal stromal tumours. J Cell Mol Med 2009; 13: 1536-1548.
[38] Eriksen AC, Sorensen FB, Lindebjerg J, Hager H, dePont Christensen R, Kjaer-Frifeldt S and Hansen TF. The prognostic value of tumour stroma ratio and tumour budding in stage II colon cancer. A nationwide population-based study. Int J Colorectal Dis 2018; 33: 1115-1124.
[39] Li L, Jiang M, Qi L, Wu Y, Song D, Gan J, Li Y and Bai Y. Pyroptosis, a new bridge to tumor immunity. Cancer Sci 2021; 112: 3979-3994.
[40] Gao L, Dong X, Gong W, Huang W, Xue J, Zhu Q, Ma N, Chen W, Fu X, Gao X, Lin Z, Ding Y, Shi J, Tong Z, Liu T, Mukherjee R, Sutton R, Lu G and Li W. Acinar cell NLRP3 inflammasome and gasdermin D (GSDMD) activation mediates pyroptosis and systemic inflammation in acute pancreatitis. Br J Pharmacol 2021; 178: 3533-3552.
[41] Zheng Z and Li G. Mechanisms and therapeutic regulation of pyroptosis in inflammatory diseases and cancer. Int J Mol Sci 2020; 21: 1456.

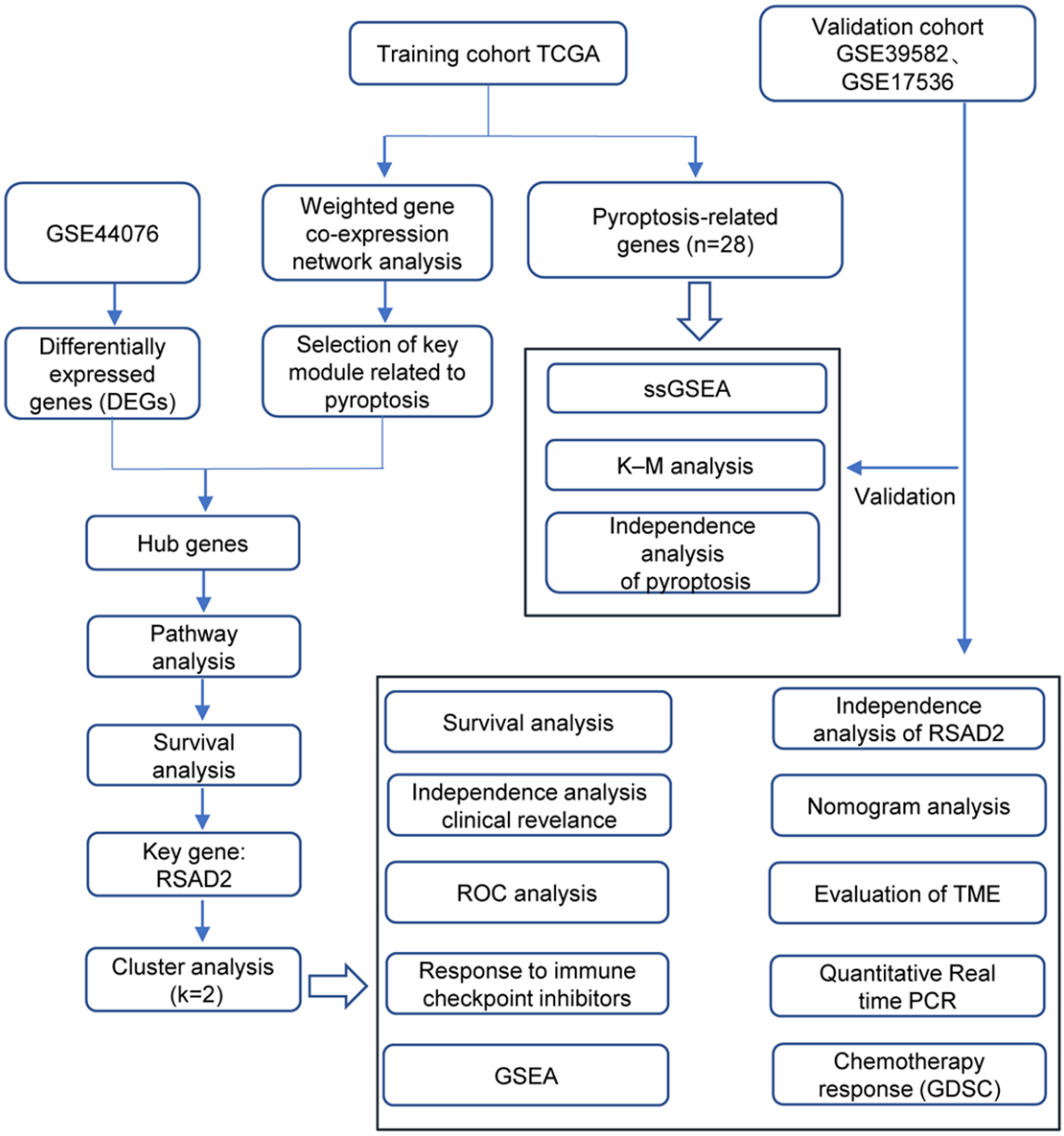

Figure S1. The flowchart of this research.

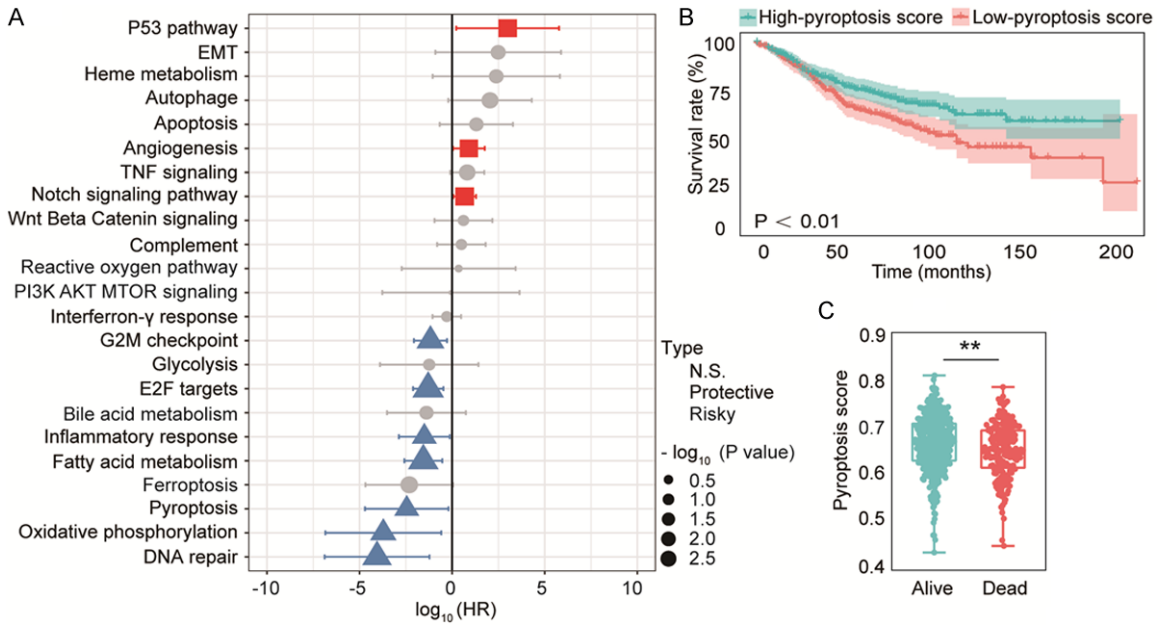

Figure S2. Identifying pyroptosis-related to CRC overall survival (OS). A. Hazard ratio (HR) of 23 cancer pathways for prognosis in the forest plot. B. Kaplan-Meier curve for samples with low pyroptosis score and high pyroptosis score. C. Differences in pyroptosis scores between dead and alive patients.

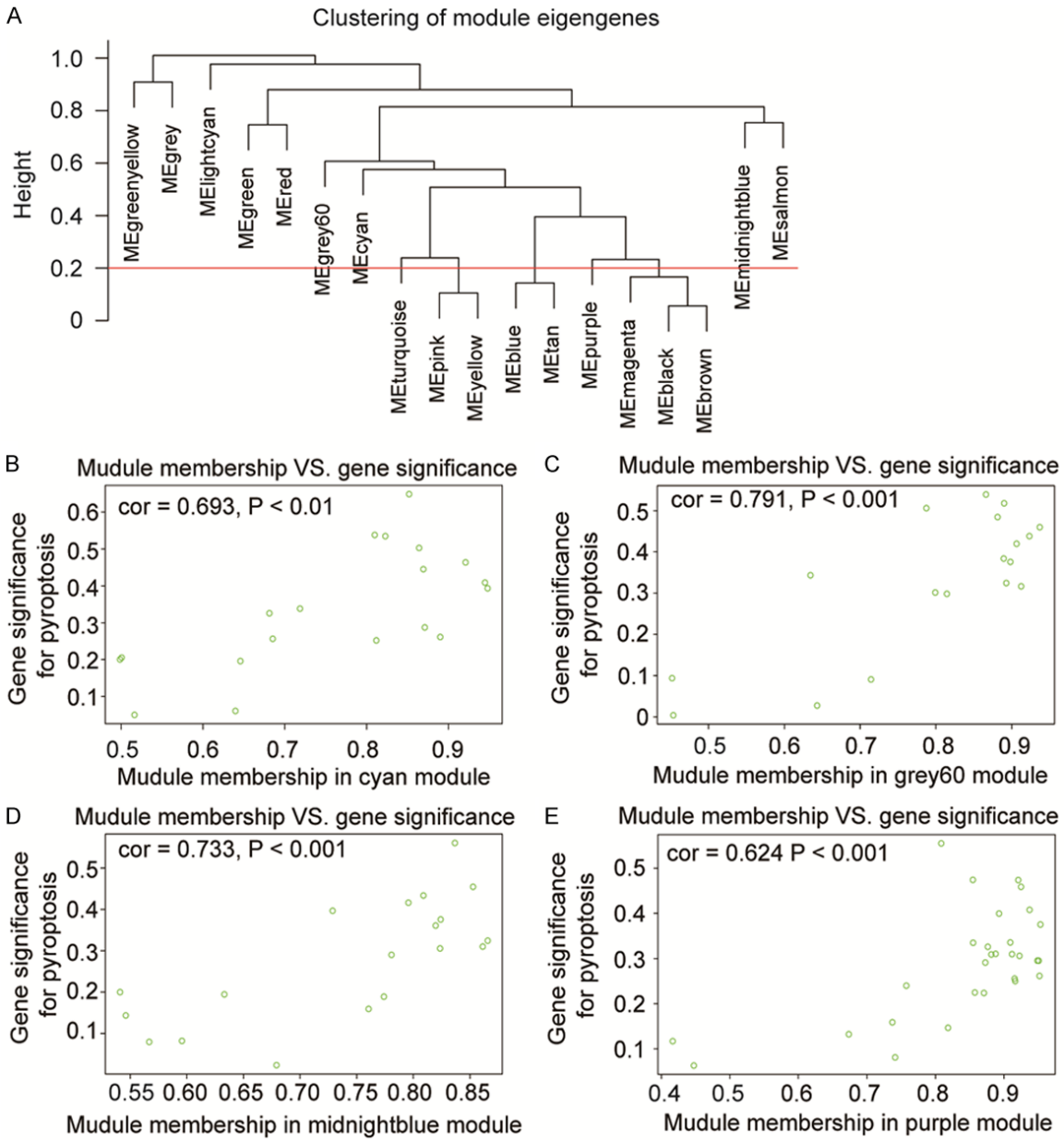

Figure S3. Selection of PGS in the TCGA. (A) The abline for clustering of modules memberships. Relevance between cyan module (B), grey60 module (C), midnightblue module (D), purple module (E) and pyroptosis.

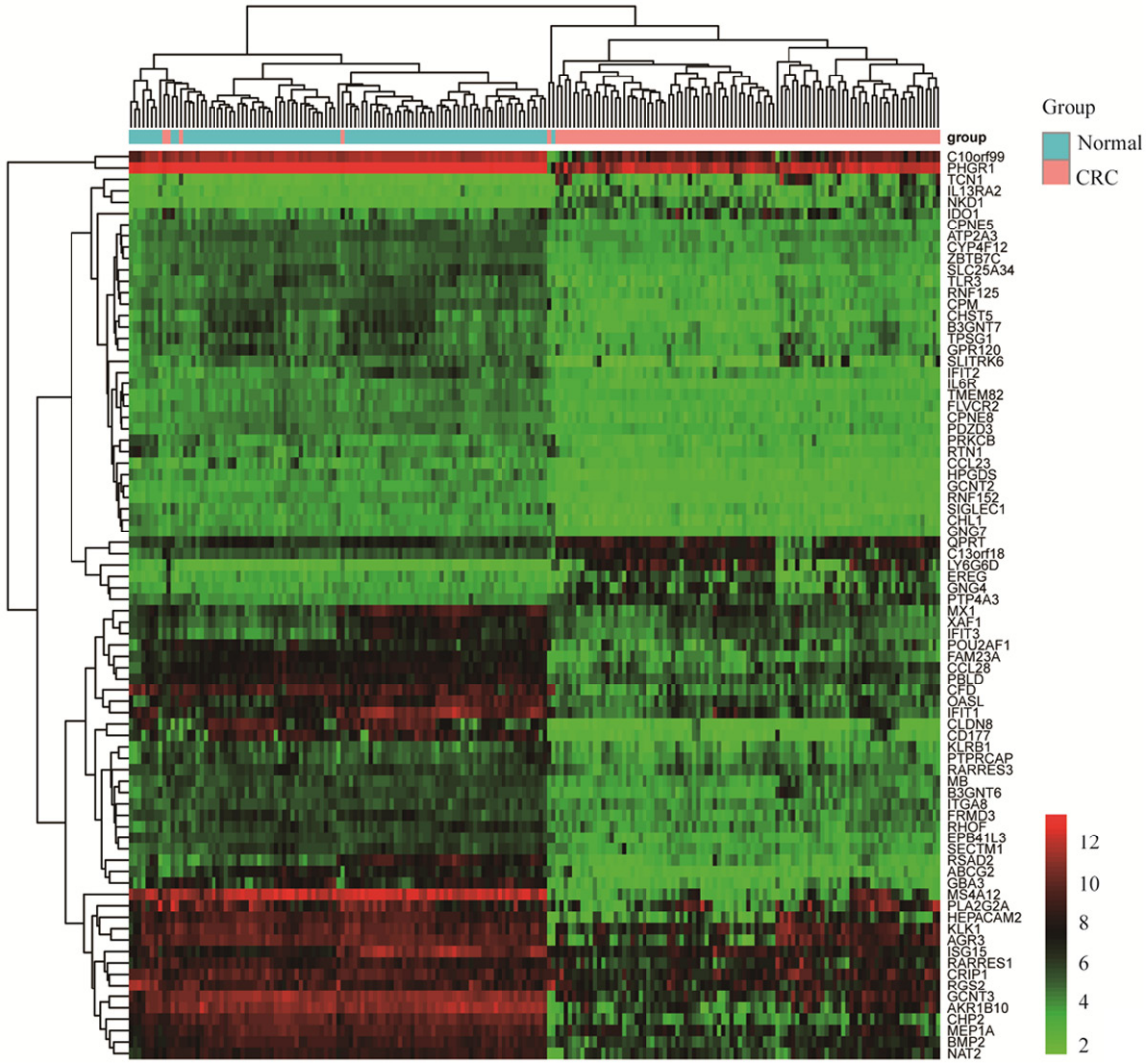

Figure S4. Hierarchical clustering heat map of top 100 hub genes using R package “pheatmap”.

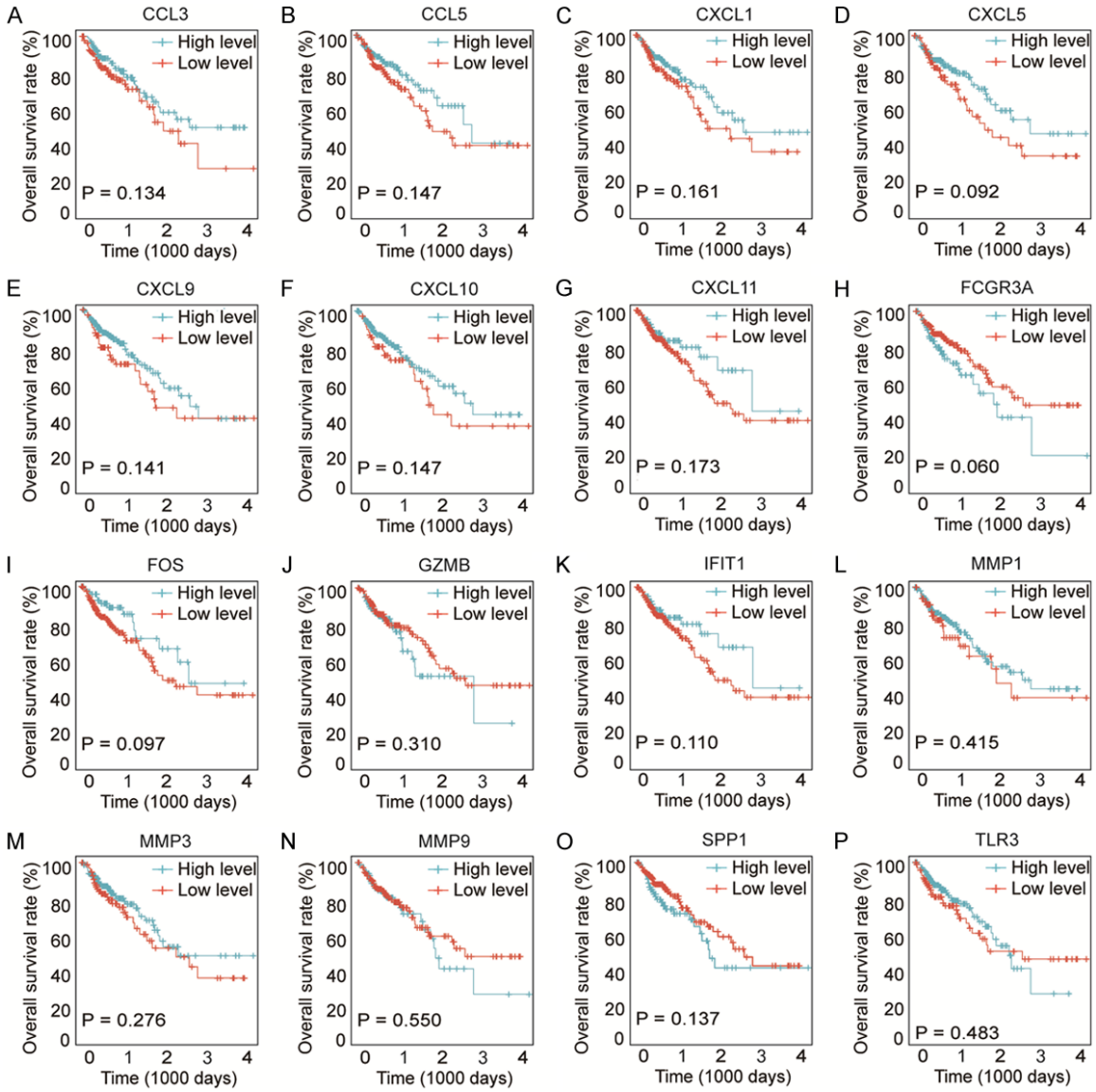

Figure S5. Kaplan-Meier survival curves of CRC samples with high (blue lines) and low (red lines) expression of hub genes. Kaplan-Meier OS curves for CCL3 (A), CCL5 (B), CXCL1 (C), CXCL5 (D), CXCL9 (E), CXCL10 (F), CXCL11 (G), FCGR3A (H), FOS (I), GZMB (J), IFIT1 (K), MMP1 (L), MMP3 (M), MMP9 (N), SPP1 (O), and TLR3 (P) in the TCGA.

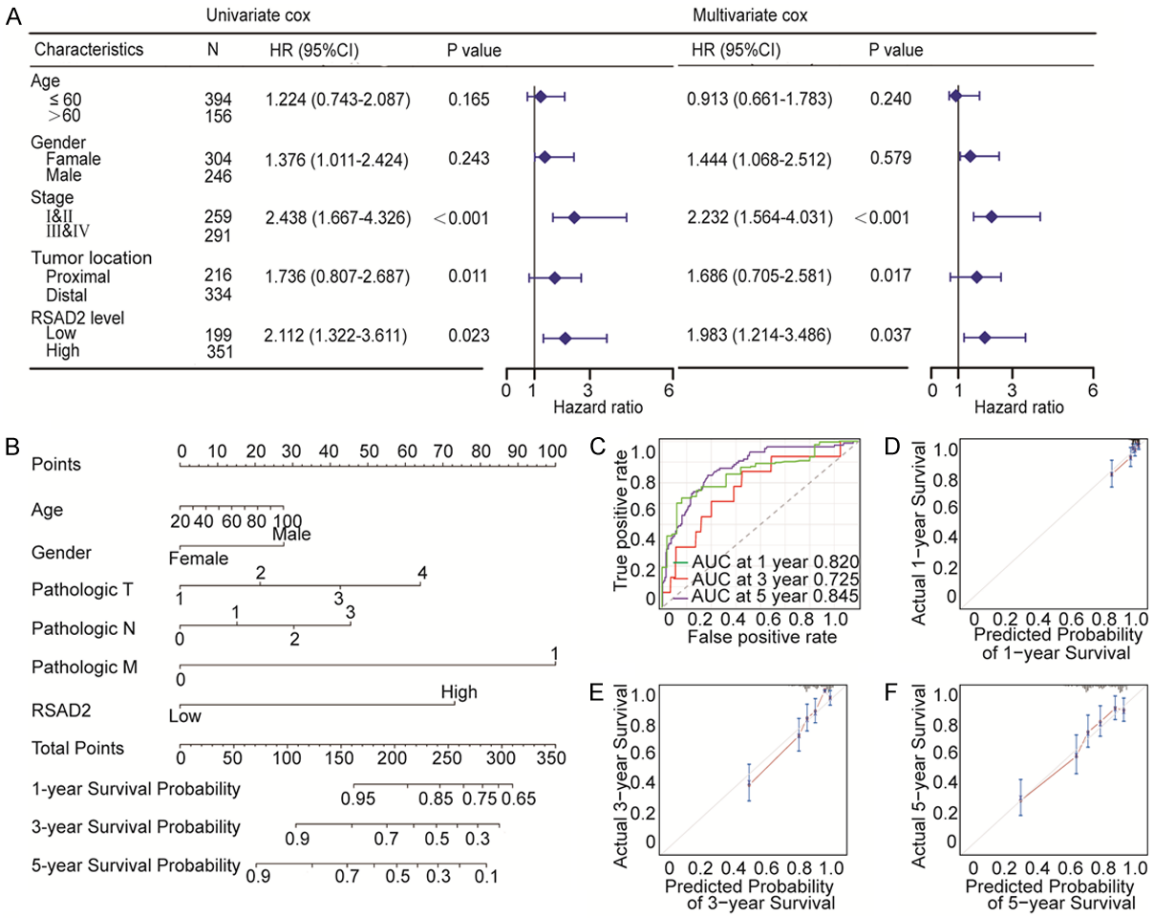

Figure S6. Validation of RSAD2 as a key gene and an independent prognostic factor of CRC. A. Univariate and multivariate Cox regression analyses of RSAD2 level combined with age, gender, tumor stage and tumor location. B. Prediction of CRC patients by the nomogram established based on multivariate Cox regression analysis. C. Time-dependent ROC curves at 1, 3 and 5 years. D-F. Comparison between actual and nomogram-predicted 1-, 3- and 5-year OS in the calibration plot.

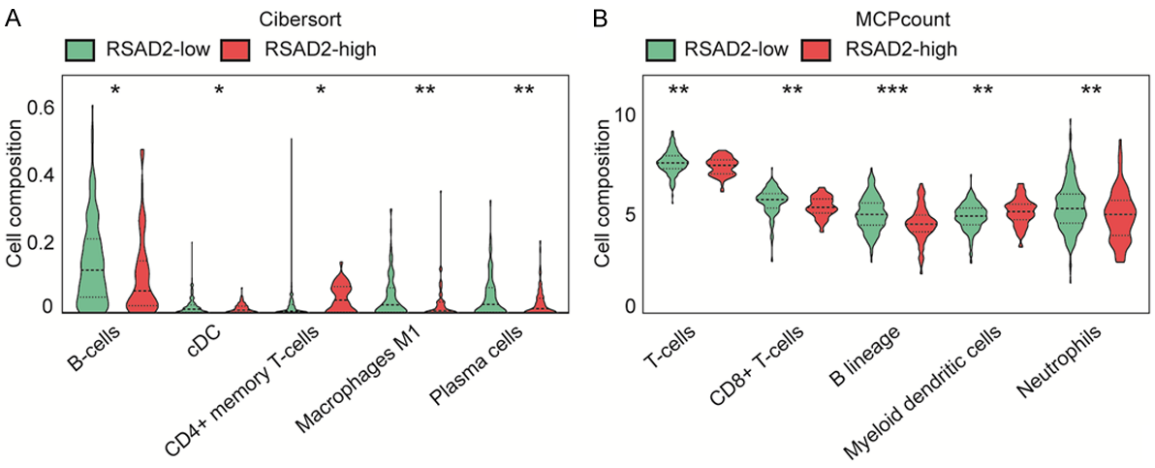

Figure S7. Evaluation of immune cells infiltration using Cibersort (A) and MCPcount (B) in RSAD2-low and RSAD2-high groups.

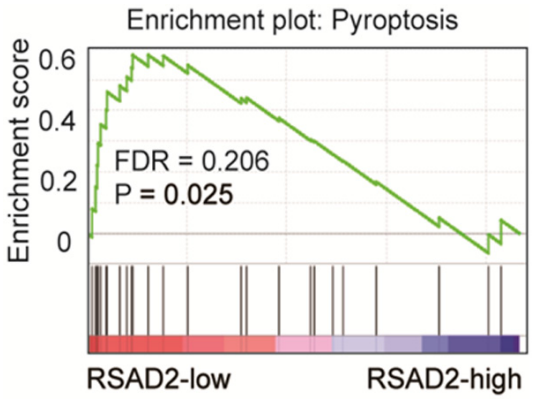

Figure S8. GSEA of pyroptosis pathway in RSAD2-low and RSAD2-high groups.